Ind. Eng. Chem. Res. **1995,** *34,* 2349−2357

Naphthalene Hydrogenation over Pt/Al_2O_3 Catalyst in a Trickle Bed Reactor

Ting-Chia Huang* and Ben-Chang Kang

Department of Chemical Engineering, National Cheng Kung University, Tainan, Taiwan, Republic of China 701

The biaromatic compound naphthalene dissolved in different volatile solvents has been hydrogenated over Pt/Al_2O_3 catalyst in a trickle bed reactor. The activity and selectivity have been investigated with various hydrogen and feed flow rates at 513 K and 5.17 MPa. The effects of partial liquid evaporization and wetting efficiency of catalyst particles on the performance of a trickle-bed reactor were studied. Experimental results and parameters calculated from the reactor model indicated that neglecting the wetting efficiency would lead to a misleading conclusion in reaction kinetics. High volatilities of feedstocks, high gas flow rate, and low liquid flow rate decrease wetting efficiencies of catalyst particles. The activity of naphthalene hydrogenation increased with increasing wetting efficiency, and the selectivity of *cis*-decalin decreased with increasing volatility of solvent.

Introduction

High aromatic content in diesel fuel lowers fuel quality and contributes significantly to the formation of undesired emissions in exhaust gases (Barry et al., 1985; Lindsay et al., 1992; Ullman, 1989). Because of the health hazards associated with these emissions, the environmental regulations governing the composition and limitations of aromatics in diesel fuels are being tightened in the developed nations.

In recent years, considerable attention has been paid to new catalysts and processes for aromatic saturation. The most famous process is conventional hydrotreating catalysts in first-stage operation and noble metal catalyst in second-stage operation. For deep aromatic saturation using a noble-metal catalyst in second stage is particularly preferred.

There is much research on the hydrogenation of aromatic compounds catalyzed by sulfided CoMo/γ-Al_2O_3 (Broderick et al., 1987; Pazter et al., 1979; Sapre and Gates, 1982, 1981) or NiW/γ-Al_2O_3 (Wilson et al., 1985; Wilson and Kriz, 1984). Numerous studies have been carried out for the low-pressure hydrogenation of benzene (or toluene) catalyzed by Pt catalysts (Basset et al.,1975; Ceckiewicz and Delmon, 1987; Orozco and Webb,1983; Gutierrez-Ortiz et al., 1993). However little information is available about the reactions of biaromatics (or polyaromatics) over supported noble metal catalysts under high pressure (Koussathana et al., 1991; Koussathana et al., 1992; Sakanishi et al., 1989). Hence hydrogenation of naphthalene over Pt/Al_2O_3 catalyst at high pressure in a trickle-bed reactor was studied in this work.

Diesel feedstock is not a single compound; it contains a large number of components. In the correlation of reaction data from the trickle-bed reactors, results are frequently presented in terms of liquid hourly space velocity (LHSV) based on liquid feed to the reactor regardless of the extent to which the various components of the feed may be vaporized within the reactor. The reactants, reaction intermediates, solvent, and products may be of significantly different volatility, and of different distribution themselves between the liquid and vapor phases. This distribution is affected not only by pressure and temperature, but also by the ratio of flow rates of gas and liquid. This ratio can thus affect the liquid and gas concentrations in contact with the catalyst (Lavopa and Satterfield, 1988; Nalitham et al., 1985).

The wetting efficiency, i.e., the fraction of external surface covered by flowing liquid, is an important factor affecting reactor performance. The flow rates of gas and liquid will affect the wetting efficiency of catalyst. In this study, the reaction of a rather nonvolatile reactant (naphthalene) and a sparingly soluble volatile reactant (hydrogen) was considered. The nonvolatile reactant is supplied primarily to the pellet from the liquid film flowing over the pellet surfaces. The volatile reactant traverses two different paths. It can dissolve into and diffuse through the liquid film to the pellet surface, or take a more direct route from the gas to the nonwetted surface. The rate of supplement of hydrogen to the nonwetted surface is much larger than on the wetted surface (Funk et al., 1991). If the feed has been more vaporized, the intraparticle of catalyst may be partially wetted, and the gas phase reaction must be considered. All these factors affect reaction conversion and product selectivity (Smith and Satterfield, 1986; Nalitham et al., 1985; Herskowitz and Mosseri, 1983; Montagna and Shah, 1975). In this study, a model is presented to quantify the effects of wetting efficiency of catalyst particle on the performance of trickle-bed reactors. The model views the trickle-bed reactor as a series of CSTR reactors interconnected with vapor−liquid equilibrium stages and is checked by experimental results.

The heat of combustion of *cis*-decalin is 38.33 MJ/M^3, and the heat of combustion *trans*-decalin is 37.15 MJ/M^3 (Weitkamp, 1968). The greater the amount of *cis*-decalin in total decalin, the higher the total heat combustion value is. Hence the higher selectivity of *cis*-decalin is desired at the same hydrogen consumption and same operating cost. In this work, not only the activity of naphthalene hydrogenation but also the selectivity of *cis*-decalin was studied experimentally for the above influential factors.

Experimental Section

Catalyst Preparation and Characterization. United Catalysts Inc. Cs-331-4 alumina particle, 25−

---

* Author to whom correspondence should be addressed.

0888-5885/95/2634-2349$09.00/0

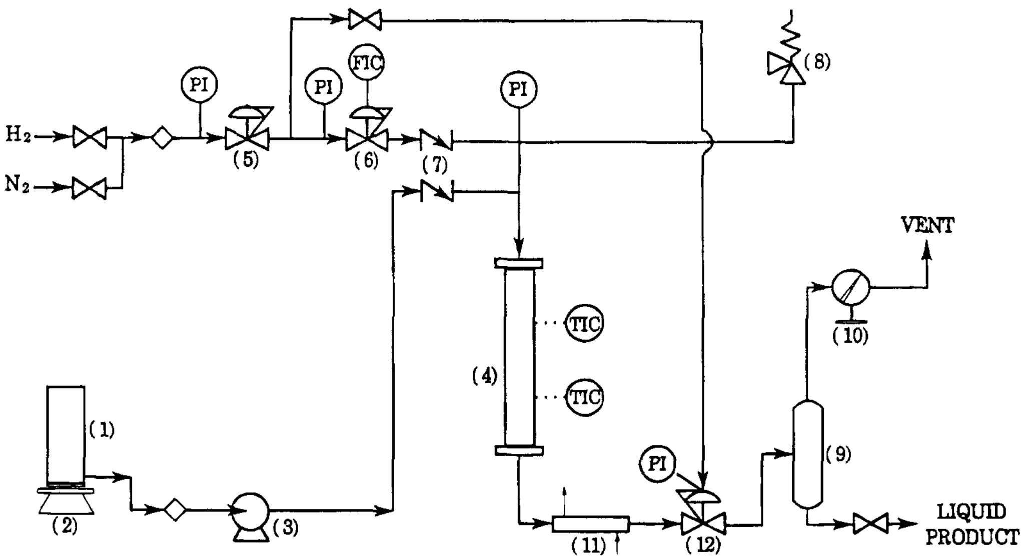

Figure 1. Simplied flow diagram of continuous hydrogenation test unit. (1) Feed tank; (2) balance; (3) feed pump; (4) reactor; (5) forward pressure regulator; (6) mass flowmeter and controller; (7) check valve; (8) safety relief valve; (9) gas–liquid separator; (10) wet-test meter; (11) cooler; (12) back-pressure regulator.

Table 1. The Physical Properties of the Employed Compounds and Reaction Products

compound	mp (K)	bp (K)
naphthalene	353.5	490.0
tetralin	242.0	480.0
trans-decalin	242.6	460.2
cis-decalin	229.7	468.7
n-octane	216.0	399.0
n-dodecane	263.0	489.0
n-hexadecane	291.0	553.0

45 mesh (355–710 μm), was used as the support of the prepared catalyst. The textural properties of support (BET surface area 198.9 m^2g^{-1}, pore volume 0.658 cm^3 g^{-1}, average pore diameter 6.58 nm) were determined by the nitrogen sorption method (Micromeritics 2400).

The method of incipient wetness impregnation of the support was employed to prepare the catalyst; i.e., γ-Al_2O_3 was impregnated with appropriate amounts of chloroplatinic acid (Merck) aqueous solution. Impregnated supports were kept in air overnight and calcined at 383 K for 4 h and then at 673 K for 4 h. The platinum metal content of the catalysts, 0.63 wt %, was determined by inductively coupled plasma–atomic emission spectrometry (Jarrell-Ash, Model 100). Pt/Cs-331-4 catalyst had the same surface area and pore volume as Cs-331-4 support (Huang and Kang, 1995). The metal dispersion, determined by CO chemisorption (Micromeritics Chemisorb 2800) (Wells, 1985), was high (0.92) in this study.

Reactants. The model compound, naphthalene (Merck, purity > 99%), was used as a reactant. Different solvents, *n*-hexadecane, *n*-dodecane, and *n*-octane (all Merck products, purity > 99.5%; main impurity is *n*-paraffin) were used to dissolve the model compound. The physical properties of reactant, solvents, and reaction products are shown in Table 1. High-purity hydrogen (99.99%, Sanfu Co.) was used in this study.

Reaction System. The bench-scale reaction system, a cocurrent downflow trickle-bed reactor, used in this study is shown in Figure 1. The reactor was heated and contolled by three electric resistors and three thermocouples, and the temperature over the the reaction zone was kept constant. The reaction temperature was monitored with three thermocouples. One of the thermocouples was set in the center of the catalyst bed; the other two were set outside the tube reactor at the top and bottom of the catalyst bed, respectively. The temperature differences between these thermocouples were less than 1.5 °C at steady state. Hence we assumed the catalyst bed was isothermal. The hydrogen gas flow rate was measured and controlled by a Brooks mass flowmeter and controller. The liquid feed was supplied by a Gasukuro Kogyo HPLC pump. The liquid and gas products from the reactor passed through a back-pressure regulator and cooled to ambient temperature in a double pipe heat exchanger before they entered the gas–liquid separation system. Liquid-sampling parts were provided immediately beneath the cooler and the separator.

The equivalent spherical diameter of the catalyst used in this study was smaller than 710 μm (25–45 mesh). The stainless steel tube reactor had an internal diameter of 11 mm and a length of 430 mm. In this study, the conversion of naphthalene hydrogenation to decalin was high. The catalyst bed was diluted with ceramic powder (45–80 mesh) to avoid dispersion effect and to obtain a homogeneous thermal distribution in the reactor (Klinken and Dongen, 1980; Tsai et al., 1991). The volume ratio of inert ceramics to catalyst was 2, and catalyst and ceramics were loaded one after another. The remaining spaces of catalyst bed at the top and the bottom of reactor were filled with ceramic powder to avoid the entrance and exit effects.

The same batch of prepared catalyst was used for all tests in this work. In each run a new mass of the fresh catalyst was loaded in the reactor; the temperature, pressure, and solvent were kept the same, but the flow rates and liquid feed composition were changed randomly. The first experimental condition was repeated in the middle and at the end of the series of experiments with the same loading of the catalyst. No significant catalyst deactivation was detected.

Catalysts were reduced in situ by H_2 at 673 K for 4 h before the feed was introduced. After reducing of the catalyst, the reactor was cooled to the desired temperature and then the reactants were introduced.

The liquid samples were withdrawn with a sampling valve from the separator and analyzed by a gas chromatograph (Carlo Erba, Model 6000) equipped with a flame ionization detector (FID) and an electronic integrator (Carle Erba, Model DP 700). A 10 m by 0.5 mm fused-silica wide-bore column, type WCOT, with liquid phase CP-SIL-5CB, was used to separate reactants and products. The chromatographic analysis was conducted under temperature-programming conditions. When one operation variable was changed, several samples were withdrawn and analyzed until steady state.

In these experiments, the mass balances, obtained from calculation of the composition and amount of input and output, were more than 99% for heavy solvent feed, but more than 98% for *n*-octane solvent feed.

Results and Discussion

Blank experiments were performed by using pure γ-Al_2O_3 as catalyst. There was no observable conversion even under more severe condition (607 K) than this study. Therefore, all the observed reactions were catalyzed by Pt/γ-Al_2O_3. It was consistent with the result of Sapre and Gates (1981). The feed of naphthalene in *n*-hexadecane solvent was run twice with fresh catalyst loaded. The conversion difference between the two was less than 1.0% (Huang and Kang, 1995). Hence experimental reproduciblity is good. There are three different kinds of hydrogenated products of naphthalene at various operation conditions. The reaction can be described as following:

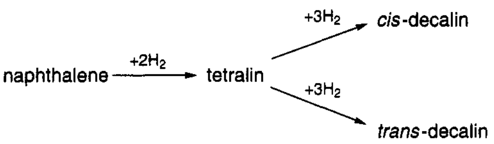

No secondary products and no cracking of solvents were observed in this study. The rate of hydrogenation of naphthalene to tetralin is 1 order higher than that of tetralin to decalin (Sapre and Gates, 1981; Wilson et al.,1985). Naphthalene was not found in the reaction product in this work. Therefore, it is assumed that naphthalene is completely hydrogenated to tetralin in the front of the catalyst bed.

Determination of the Wetting Efficiency. The rate for establishing vapor–liquid equilibrium, which typically has a time constant of the order of seconds, is much faster than the rate of hydroprocessing reaction whose time constant typically is of the order of hours. Thus, for small increments of reactor contact time, a flash process could be considered to occur. Component partial pressures can be estimated by assuming that vapor–liquid equilibrium is established at all points in the catalyst bed. With this assumption, an appropriate vapor–liquid equilibrium can be used in a flash calculation to determine species mole fractions. The reactor model suggeested by Lavopa and Satterfield (1988) is modified and used in this work.

Mathematically the reactor is modeled as *N* stages in series with each stage containing an equilibrium flash and a differential reactor modeled as a CSTR, as shown in Figure 2. Figure 2 represents any of the stages from 1 to *N*; liquid feed L_{i-1} and vapor stream V_{i-1} enter stage *i* with known compositions. A flash calculation determines the equilibrium mole fractions which satisfy the following mass balance equation:

$$L'_i x'_{ij} + V'_i y'_{ij} = L_{i-1}x_{i-1,j} + V_{i-1}y_{i-1,j} \tag{1}$$

for each component *j*. Using the calculated equilibrium partial pressures $y'_{ij}P$, mole fraction x'_{ij}, and the reaction kinetics, the conversion in reaction zone *i* can be determined.

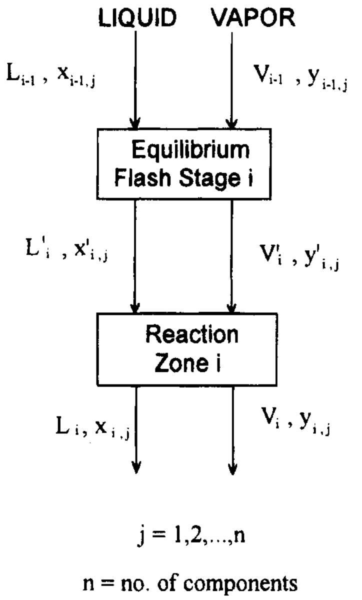

Figure 2. Mathematical model.

The reaction rate given by LaVopa and Satterfield (1988) assumed complete wetting of the catalyst particles, used vapor phase kinetics, and is shown in the following:

$$\frac{d(1-X)}{dt} = -kP_0(1-X)P_H \tag{2}$$

From the experimental results, the reactor model (eq 2) failed in this study due to the high activity of Pt/Al_2O_3 catalyst and the partial wetting of catalyst particle. A reaction rate suggested by Ruecker and Akgerman (1987) was modified and is given by

$$-\frac{N_0\,d(1-X)}{dW} = f\eta_l k_l C_0(1-X)C_H + (1-f)\eta_g k_g P_0(1-X)P_H \tag{3}$$

Integration over the catalyst bed gave

$$W = -\int_1^{1-x_f} \frac{N_0\,d(1-X)}{f\eta_l k_l C_0(1-X)C_H + (1-f)\eta_g k_g P_0(1-X)P_H} \tag{4}$$

Wetting efficiencies are determined from experimental trickle-bed data by eq 4 provided $\eta_l k_l$ and $\eta_g k_g$ are known. This approach assumes that the wetting efficiency remains constant throughout the reactor.

If the reaction is performed under conditions such that no liquid phase exists, then $f = 0$ and eq 4 reduces to

$$\eta_g k_g = -\frac{1}{W}\int_1^{1-x_f} \frac{N_0\,d(1-X)}{P_0(1-X)P_H} \tag{5}$$

Hence a simple integration yields $\eta_g k_g$. A value for $\eta_l k_l$ can be obtained in a similar manner by performing an experiment in a liquid-full reactor or by using a trickle-bed reactor at high enough liquid flow rates to ensure complete liquid coverage of the catalyst. In either case $f = 1$ and eq 4 reduces to

$$\eta_l k_l = -\frac{1}{W}\int_1^{1-x_f} \frac{N_0\, d(1-X)}{C_0(1-X)C_H} \qquad (6)$$

The value of the wetting efficiency, f, can now be obtained from eq 4 for trickle-bed experiments provided that the temperature, pressure, and catalyst bed are the same as those used to determine $\eta_l k_l$ and $\eta_g k_g$.

Phase Equilibrium Calculation. From the experimental studies here a relatively low concentration of reactant was used and hydrogen consumption was kept below 10%. Thus vapor–liquid distribution coefficients could be simplified further to include only the initial stage. The equilibrium flash calculation was used to determine the equilibrium mole fractions in initial reaction stage for each set of reactor conditions. Each component j in the initial reaction stage satisfies the following mass balance equation:

$$L_0 x_{0,j} + V_0 y_{0,j} = L'_1 x'_{1,j} + V'_1 y'_{1,j} \qquad (7)$$

where $j = 1, 2, ..., n$ and n = the number of components. In this study, 1 is tetralin, 2 is solvent, and 3 is hydrogen.

Let

$$z_j = (L_0 x_{0,j} + V_0 y_{0,j})/(L_0 + V_0) \qquad (8)$$

and

$$v = V'_i/(L_0 + V_0) \qquad (9)$$

From eq 7

$$y_{1,j} = z_j K_{1,j}/(1 + v(K_{1,j} - 1)) \qquad (10)$$

where

$$K_{i,j} = y_{i,j}/x_{i,j} \qquad (11)$$

Since $\sum_j y_{i,j} = 1$, the sum of eq 10 gives

$$\sum_j z_j K_{1,j}/(1 + v(K_{1,j} - 1)) = 1 \qquad (12)$$

In eq 12, $K_{1,j}$ are known and z_j are calculated from eq 8. Using Newton's method, v can be calculated. Then $y_{1,j}$ values can be calculated from eq 10 and $x_{1,j}$ from eq 11.

The vapor–liquid equilibrium data of the binary systems tetralin–hydrogen, decane–hydrogen, and hexadecane–hydrogen, reported by Chao et al. (1980), were used in this study. The K values were affected strongly by the reaction temperature and pressure, but weakly by the composition. Approximate K values are assumed to be independent of composition in this study (Nalitham et al., 1985). Experimental K values for naphthalene, n-octane, and n-dodecane are not available in the literature. As an approximation, the K value of naphthalene is estimated from the K value of tetralin and its vapor pressure by assuming that the K values for naphthalene and tetralin are proportional to their vapor pressures (Ohe, 1976; Boublik et al., 1984). The K values of n-octane and n-dodecane are obtained with the same method from the K value of n-decane and their vapor pressures. Experimental K values of several binary systems and calculated K values are listed in Table 2. The calculated K value of n-hexadecane is nearly equal to the experimental K value, as shown in Table 2.

Table 2. Experimental K Values for Several Binary Systems and Calculated K Values for Single Compounds

component	exptl K value[a]	compound	calcd K value
hydrogen	10.69	n-octane	0.2736
n-hexadecane	0.00770		
		n-dodecane	0.04369
hydrogen	10.536		
n-decane	0.10637	naphthalene	0.0411
hydrogen	26.557	n-hexadecane	0.00826
tetralin	0.0506		

[a] From Chao et al. (1980).

Table 3. Components of Mole Fraction at Liquid–Vapor Equilibrium in the Initial Reaction Region for n-Octane Solvent System at Different Hydrogen Flow Rates, 513 K, and 5.17 MPa

H_2 flow rate (mL of H_2/mL of liq)	liquid mole fraction x_1	x_2	x_3	vapor mole fraction y_1	y_2	y_3	L_i/L_0
250	0.130	0.807	0.063	0.007	0.221	0.772	0.597
500	0.232	0.703	0.065	0.012	0.192	0.796	0.182
600	0.285	0.649	0.066	0.014	0.178	0.808	0.070
650	0.311	0.623	0.066	0.016	0.170	0.814	0.024
1000				0.012	0.119	0.870	0.000

Table 4. Components of Mole Fraction at Liquid–Vapor Equilibrium in the Initial Reaction Region for n-Dodecane Solvent System at Different Hydrogen Flow Rates, 513 K, and 5.17 MPa

H_2 flow rate (mL of H_2/mL of liq)	liquid mole fraction x_1	x_2	x_3	vapor mole fraction y_1	y_2	y_3	L_i/L_0
250	0.117	0.805	0.078	0.006	0.035	0.959	0.986
500	0.116	0.806	0.078	0.006	0.035	0.959	0.872
750	0.114	0.808	0.078	0.006	0.035	0.959	0.758
1000	0.112	0.810	0.078	0.006	0.035	0.959	0.644
2000	0.106	0.815	0.078	0.005	0.036	0.959	0.188
2250	0.105	0.817	0.078	0.005	0.036	0.959	0.074
3000				0.004	0.029	0.967	0.000

Table 5. Components of Mole Fraction at Liquid–Vapor Equilibrium in the Initial Reaction Region for n-Hexadecane Solvent System at Different Hydrogen Flow Rates, 513 K, and 5.17 MPa

H_2 flow rate (mL of H_2/mL of liq)	liquid mole fraction x_1	x_2	x_3	vapor mole fraction y_1	y_2	y_3	L_i/L_0
250	0.138	0.782	0.080	0.007	0.006	0.987	1.000
500	0.126	0.794	0.080	0.006	0.006	0.988	1.000
750	0.115	0.804	0.080	0.006	0.007	0.988	0.964
1000	0.105	0.814	0.080	0.005	0.007	0.988	0.923
2000	0.080	0.839	0.080	0.004	0.007	0.989	0.790
3000	0.064	0.856	0.081	0.003	0.007	0.990	0.664

According to eqs 10–12, the mole fraction of components in different phases and the fraction of liquid feed vaporized in the initial stage of the reactor were calculated. The calculated results are shown in Tables 3–5. They indicate that the lighter the solvent is in the feed, the greater the amount of liquid feed is vaporized. A greater amount of liquid feed is vaporized with increasing hydrogen flow rate. However the concentration of hydrogen in the liquid phase is nearly independent of the hydrogen flow rate. The concentrations of hydrogen in the liquid phase and vapor phase are the highest when hexadecane is used as a solvent. By increasing the hydrogen flow rate, the concentrations of tetralin in the liquid and vapor phase increase when the octane is used as a solvent, and are nearly constant when the dodecane is used as a solvent, but decrease when the hexadecane is used as a solvent.

Effects of the Hydrogen Flow Rate on the Performance of the Reactor. Experiments were carried out to study how the influence of the volatilites of feed components on the conversion and selectivity at con-

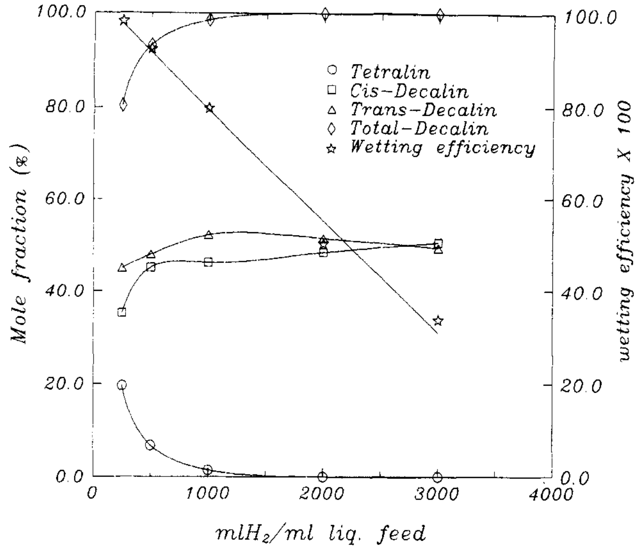

Figure 3. Effect of hydrogen flow rate on activity and selectivity of naphthalene hydrogenation in n-hexadecane at 513 K, 5.17 MPa, and 2.7 LHSV.

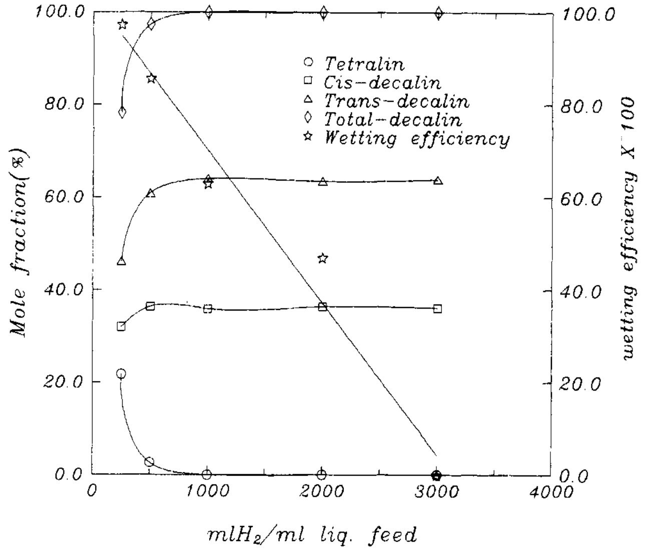

Figure 4. Effect of hydrogen flow rate on activity and selectivity of naphthalene hydrogenation in n-dodecane at 513 K, 5.17 MPa, and 2.7 LHSV.

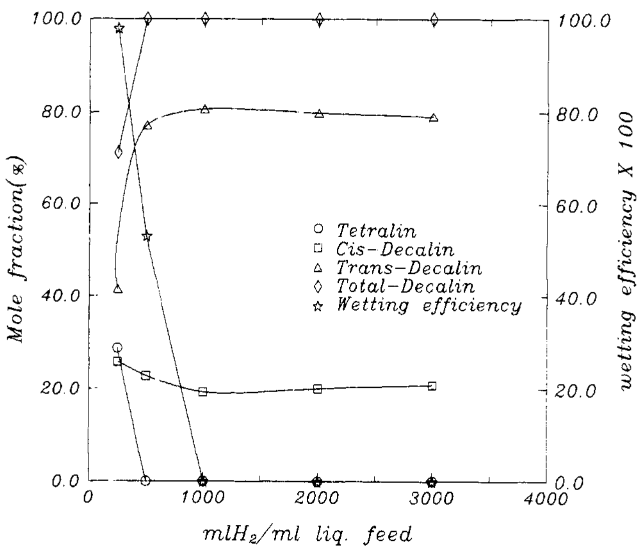

Figure 5. Effect of hydrogen flow rate on activity and selectivity of naphthalene hydrogenation in n-octane at 513 K, 5.17 MPa, and 2.7 LHSV.

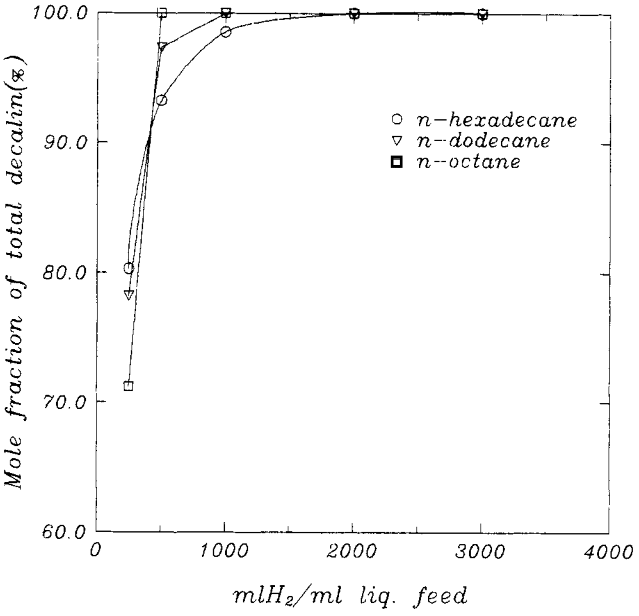

Figure 6. Influence of volatility of solvent on naphthalene hydrogenation activity at 513 K and 5.17 MPa.

stant LHSV and liquid feed composition (0.576 mol of naphthalene/L) but different hydrogen flow rates. Naphthalene, dissolved respectively in n-hexadecane, n-dodecane, and n-octane, has been hydrogenated, and the results are shown in Figures 3–6. The reaction conditions were 513 K, 5.17 MPa, and LHSV 2.7 h^{-1} (volume of liquid feed/volume of catalyst /hour) with 4 g of catalyst. The rate of hydrogenation increased with increasing hydrogen flow rate. The results were not coincident with those of Nalitham et al. (1985) and Lavopa and Satterfield (1988). According to the reactor model (eq 2) and the data of vapor phase mole fraction in Tables 3–5, the rate of hydrogenation would be decreased for n-octane and n-hexadecane solvent feeds with increasing hydrogen flow rate. The reactor model (eq 2) was based on the assumption of completely wetting catalyst particle that was not appropriate to this study. Therefore, the experimental result was opposite what the model (eq 2) expected when the liquid feed was not completely vaporized in the reactor.

According to the results of Herskowitz and Smith (1983), the wetting efficiency of the catalyst particles in this study was lower than 1 at low liquid flow rate, even if the catalyst bed was diluted by inert (Klinken et al.,1980) to increase the wetting efficiency. As the liquid flow rate was insufficient to wet the entire catalyst surface, the volatile reactant (hydrogen) proceeded to enter the catalyst pores through the nonwetted part. With a subsequent increase of the supply rate of the gaseous reactant, the rate of reaction increased as shown in Figures 3–6. This phenomenon is the effectiveness enhancement by partial wetting (Funk et al., 1991; Harold and Ng, 1987).

If hydrogen to liquid feed ratio is larger than 1000 cm$^3_{\rm N}$/cm^3, no liquid feed is present at this condition for the n-octane–naphthalene feed system, as shown in Table 3. Hence, a value of $\eta_g k_g$ = 10.03 L^2/(mol·g of catalyst·min) is obtained from the exit conversion by using eq 5. The liquid flow rate is probably not high enough to ensure complete liquid coverage at even the lowest hydrogen flow rate. None of the experimental data points can be directly used in eq 6 to evaluate $\eta_l k_l$. An estimate value of $\eta_l k_l$ is obtained by using a hypothetical data point based on the experimental

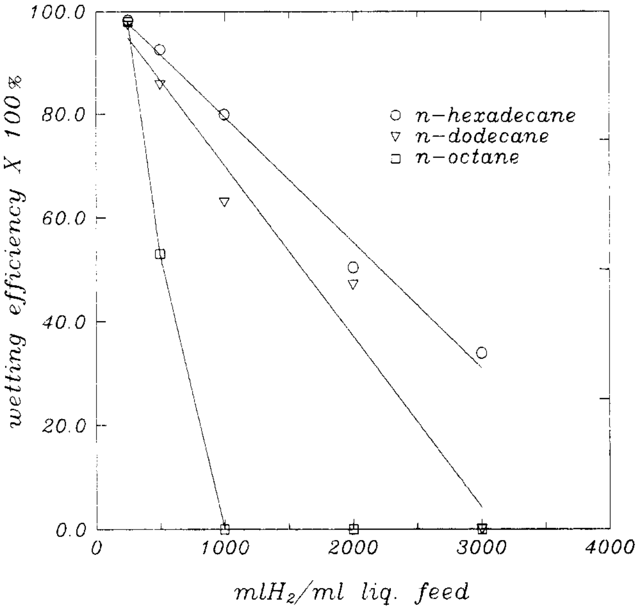

Figure 7. Effect of volatility of solvent on wetting efficiency at 513 K and 5.17 MPa.

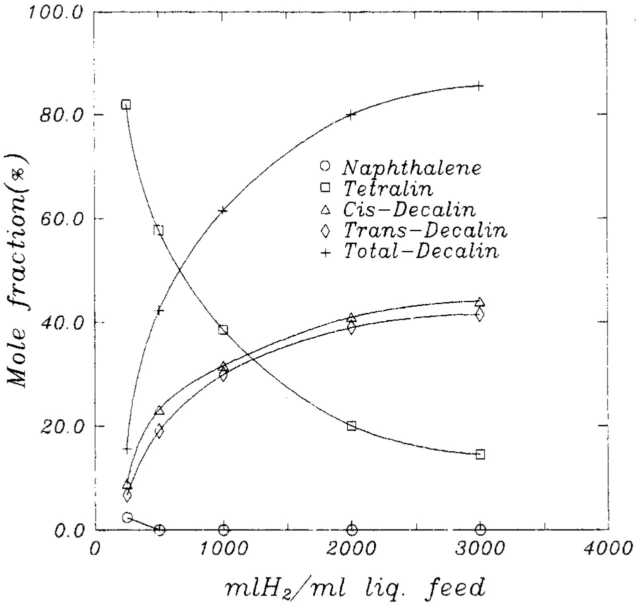

Figure 8. Effect of hydrogen flow rate on of naphthalene hydrogenation activity in *n*-hexadecane at 513 K, 5.17 MPa, and 10.8 LHSV (1 g of catalyst).

results as the method used by Ruecker and Akgerman (1987). Hence, a value of $\eta_l k_l$ = 0.039 L^2/(mol·g of catalyst·min) is obtained.

By appling the above reactor model (eq 4), the data in Tables 3–5, and experimental tetralin conversion, the wetting efficiencies were calculated and shown are in Figures 3, 4, 5, and 7. The wetting efficiency was decreased with increasing hydrogen flow rate. Herskowitz and Mosseri (1983) reported that the wetting efficiency decreased with increasing gas flow rate, especially at low liquid rates. Specchia and Baldi (1978) and Sicardi et al. (1981) found an opposite trend. In this study, the vaporization fraction of liquid feed increased with the increasing of hydrogen flow rate. Therefore, the actual liquid flow rate decreased and the wetting efficiency decreased with increasing hydogen gas flow rate. When the hydrogen flow rate increased, the nonwetted part of the catalyst and the rate of hydrogen transfer were increased. Hence the rate of hydrogenation of naphthalene increased as shown in Figures 3–6.

At the same hydrogen flow rate, a greater amount of the light solvent in the liquid feed was vaporized than the heavy solvent. The lighter the solvent of feed was, the lower the wetting efficiency was, as shown in Figure 7. The nonwetted part of the catalyst and the rate of hydrogen transfer were increased, and more of the hydrogenation reaction occurred on the nonwetting part of the catalyst. Therefore, the rate of hydrogenation of naphthalene was the fast for the feed with the lowest boiling point of solvent (octane), except at the lowest hydrogen flow rate (250 mL of H$_2$/mL of liquid feed). Because of the complete saturation of aromatics at the high hydrogen flow rate, the rate of naphthalene hydrogenation was not increased more by the increasing hydrogen flow rate in Figures 3–6.

Because more liquid was vaporized for the feed with light solvent, the hydrogenation rate increased, more *cis*-decalin isomerized to the trans form, and the partial pressure of hydrogen decreased in the reactor. According to the results of Huang and Kang (1995), the selectivity of *cis*-decalin increased by decreasing space time or by increasing hydrogen partial pressure at the fully hydrogenated naphthalene. Therefore, the *cis*-decalin selectivity of the feed with light solvent was lower than the feed with heavy solvent, at the fully saturated condition, as shown in Figures 3–5.

When the hydrogen flow rate was too high, the light solvent of feed was nearly completely vaporized and most reactions occurred in the vapor phase. For the octane as the solvent of feed, when the hydrogen flow rate was higher than 1000 mL of H$_2$/mL of liquid, all liquid feeds were vaporized and the space time of naphthalene in gas phase was decreased due to increasing hydrogen flow rate. In this case, the reactor model (eq 2) could be applied, and due to decreasing residence time and the reaction conversion there would be a small decrease with increasing hydrogen flow rate. Therefore, the selectivity of *cis*-decalin was increased a little with increasing hydrogen flow rate, as shown in Figure 5.

For the hexadecane as a solvent of feed, with increasing hydrogen flow rate, the amount of tetralin vaporized was increased, but the space time of tetralin in vapor phase was decreased. At fully hydrogenated naphthalene, the selectivity of *cis*-decalin was increased a little by increasing hydrogen flow rate, as shown in Figure 3. In Figure 4, for dodecane as a solvent, its volatility nearly equal to that of tetralin, the effect of decreasing space time of tetralin in the vapor phase by increasing hydrogen flow rate was canceled by increasing space time of tetralin in the liquid phase. Therefore, the selectivity of *cis*-decalin was not affected by the hydrogen flow rate at complete saturation of naphthalene.

To check the reactor model (eq 4), the catalyst amount was decreased from 4 to 1 g with hexadecane as a solvent of feed, and flow rates and other conditions kept constant. The effectiveness enhancement by the partial wetting was clearer in Figure 8, and the wetting efficiency was calculated in Figure 9. When the hydrogen flow rate increased, the wetting efficiency decreased and the hydrogenation rate increased as the result of above. Even though the hydrogen flow rate increased to 3000 mL of H$_2$/mL of liquid feed, the reaction rate still increased, but approached a steady value due to the reaction controlled by the diffusion of naphthalene or the surface reaction or the decreasing mole fraction in the liquid and vapor phases. Although two different

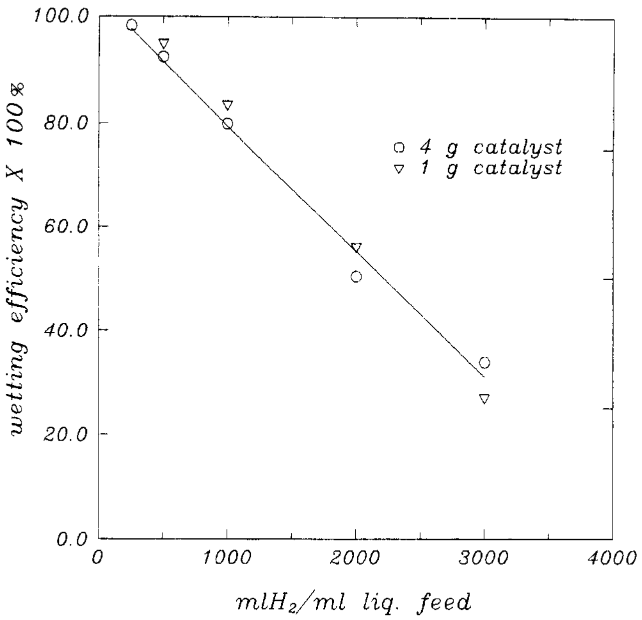

Figure 9. Comparison of the wetting efficiencies of different amounts of catalysts at 513 K, 5.17 MPa, and the same feed flow rates.

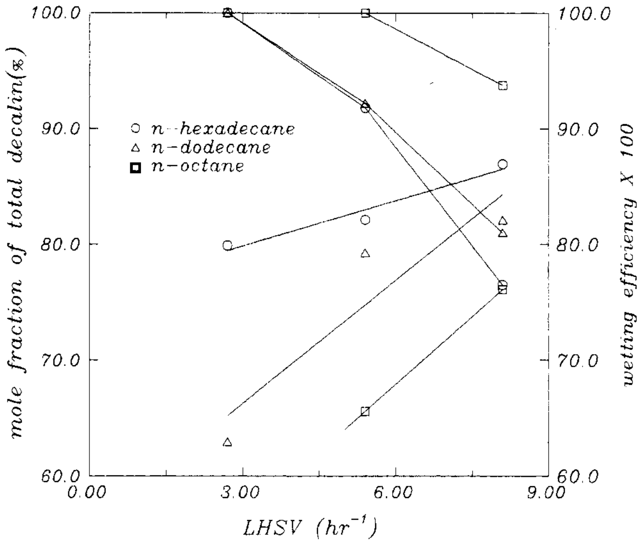

Figure 10. Effect of liquid flow rate on naphthalene hydrogenation activity at 513 K, 5.17 MPa, and 300 mL of H_2/min.

catalyst amounts were used with different reaction conversion, their wetting efficiencies, calculated by eq 4, were similar at the same feed flow rates and reaction conditions, as shown in Figure 9. Hence the reactor model (eq 4) suggested by us was reasonable. To quantify the effect of wetting efficiency on the selectivity is complex and will be done in the future.

Effect of Liquid Flow Rate on the Performance of the Reactor. Experiments were carried out to establish the effects of the presence of an inert solvent and liquid feed flow rate on the wetting efficiency, reaction conversion, and product selectivity. A series of feeds were prepared to keep the molar flow rates of hydrogen and naphthalene constant when the liquid feed flow rate was varied. Figure 10 shows the naphthalene hydrogenation activity, and Table 6 shows the selectivity of *cis*-decalin at different liquid feed flow rates with different solvents *n*-hexadecane, *n*-dodecane, and *n*-octane. The reaction conditions were kept constant at 513 K, 5.17 MPa, constant hydrogen (300 mL/min) and naphthalene flow rates, and different LHSVs of 2.7 (0.576 mol of naphthalene/L), 5.4, and 8.1 h^{-1}.

Table 6. Selectivity of *cis*-Decalin in Different Solvents at Various Liquid Feed Flow Rates

liq feed flow rate (mL/min)	hexadecane	dodecane	octane
0.32	0.846	0.618	0.326
0.64	1.158	1.048	0.705
0.96	1.420	1.384	1.044

Table 7. Mole Fraction of Components at Liquid−Vapor Equilibrium in the Initial Reaction Region for *n*-Octane Solvent System at Different Liquid Flow Rates

liquid feed flow (mL/min)	liquid mole fraction x_1	$x2$	x_3	vapor mole fraction y_1	y_2	y_3	L_i/L_0
0.32				0.012	0.119	0.870	0.000
0.64	0.173	0.752	0.075	0.007	0.206	0.787	0.081
0.96	0.073	0.854	0.073	0.003	0.234	0.763	0.297

Table 8. Mole Fraction of Components at Liquid−Vapor Equilibrium in the Initial Reaction Region for *n*-Dodecane Solvent System at Different Liquid Flow Rates

liquid feed flow (mL/min)	liquid mole fraction x_1	x_2	x_3	vapor mole fraction y_1	y_2	y_3	L_i/L_0
0.32	0.112	0.810	0.078	0.006	0.035	0.959	0.644
0.64	0.061	0.860	0.078	0.003	0.038	0.959	0.847
0.96	0.042	0.880	0.078	0.002	0.038	0.959	0.924

Table 9. Mole Fraction of Components at Liquid−Vapor Equilibrium in the Initial Reaction Region for *n*-Hexadecane Solvent System at Different Liquid Flow Rates

liquid feed flow (mL/min)	liquid mole fraction x_1	x_2	x_3	vapor mole fraction y_1	y_2	y_3	L_i/L_0
0.32	0.105	0.814	0.080	0.005	0.007	0.988	0.923
0.64	0.066	0.854	0.081	0.003	0.007	0.990	1.000
0.96	0.048	0.871	0.081	0.002	0.007	0.990	1.000

As the liquid flow rate was increased, the concentration of naphthalene, the residence time of liquid, and the nonwetted parts of the catalyst were decreased. All the factors reduced the rate of hydrogenation, as shown in Figure 10. LaVopa and Satterfield (1988) had the same result. Using eqs 10−12 and K values in Table 2, the mole fraction of components and the fraction of liquid feed vaporized in the initial reaction stage of the reactor were calculated for the various liquid feed flow rates with different solvents, and are shown in Tables 7−9. According to the reactor model (eq 4), the wetting efficiencies were calculated, as shown in Figure 10. The wetting efficiency decreased with increasing liquid flow rate, the same trend as noted by Sicardi et al. (1981) and Satterfield (1975).

The amount of vaporized light solvent was greater than the amount of heavy solvent at the same liquid and hydrogen flow rate. Hence the wetting efficiency of feed with light solvent was lower than the feed with heavy solvent. The concentration of tetralin in liquid, the mean residence time of the remaining liquid, and the nonwetting part of the catalyst for the feed with light solvent system were larger than those for the feed with heavy solvent. However, the hydrogen partial pressure and the concentration of hydrogen in the liquid for the reaction system of the feed with light solvent were lower than that of the feed with heavy solvent. The former effects, particularly the nonwetting part of the catalyst, are more dominant than the latter. The net result is obviously that the hydrogenation rate of the feed with light solvent is higher than the feed with heavy solvent, as shown in Figure 10. The low hydrogen partial pressure in the reaction system with the feed with light solvent and long residence time of the residual liquid were unfavorable to the selectivity of *cis*-decalin (Huang and Kang, 1995). Therefore, the lighter the solvent of feed was, the lower the selectivity of *cis*-decalin was in the reaction products. These coincide with the results showing in Figure 10 and Table 6.

Conclusion

The impact of partial external wetting and liquid-vapor phase equilibrium on the catalyst performance have been investigated using a packed-bed trickling flow reactor. When the gas-to-liquid flow ratio increased, the wetting efficiency of catalyst particle decreased, and the hydrogenation conversion increased. The wetting efficiency could be calculated from the reactor model (eq 4). The wetting efficiency deceased with increasing gas flow rate but increased with increasing liquid flow rate. The lighter the liquid feed was, the greater the amount of vaporized feed was and the lower the wetting efficiency was. When the liquid flow rate increased, the rate of hydrogenation should be decreased due to the increasing the wetting efficiency. The conversion and selectivity of products were also influenced by the relative volatilities of feed components. These effects were significant, when the relative volatilities of reactant and solvent were high. The reactor model (eq 4) could be reasonably applied to the experimental results.

For a purely catalytic reaction, the conversion and selectivity of a reaction in a trickle-bed reactor depend not only on LHSV, intrinsic kinetics, and feed concentrations, but also on the relative volatilities of feed components and relative flow rate. Because the partial wetting phenomenon exists in the bench-scale trickle-bed reactor, one must be careful of applying the results from the laboratory to a commerical plant.

Acknowledgment

The authors wish to express their gratitude for the support of this work by the Refining and Manufacturing Reseach Center of Chinese Petroleum Corporation.

Nomenclature

C_0 = initial limiting reactant concentration in the liquid phase
C_H = initial hydrogen concentration in the liquid phase
f = wetting efficiency
K = vapor–liquid distribution coefficient, y/x
k = reaction rate constant
L = molar flow rate of liquid, mol/min
N_0 = initial molar flow rate of limiting reactant
P_0 = initial reactant partial pressure, MPa
P_H = initial hydrogen partial pressure, MPa
V = molar flow rate of gas, mol/min
W = amount of catalyst, g
X = fraction conversion of reactant
x = mole fraction in liquid phase
y = mole fraction in gas phase
η = effectiveness factor

Subscripts

g = gas
l = liquid
H = hydrogen

Literature Cited

Barry, E. G.; McCabe, L. J.; Gerke, D. H.; Perez, J. M. Heavy Duty Diesel Engine/Feuls Combustion Performance and Emissions—A Cooperative Research Program. *SAE Pap.* **1985**, No. 852078.

Basset, J. M.; Dalmai-Imelik, G.; Primet, M.; Mutin R. A Study of Benezene Hydrogenation and Identification of the Adsorbed Species with Pt/Al_2O_3 Catalysts. *J. Catal.* **1975**, *37*, 22–36.

Boublik, T.; Fried, V.; Hala, E. *The Vapor Pressures of Pure Substances*; Elsevier: Amsterdam, 1984.

Broderick, D. H.; Spare, A. V.; Gates, B. C.; Kwart, H.; Schuit, G. C. A. Hydrogenation of Aromatic Compounds Catalyzed by Sulfided CoO-MoO_3/γ-Al_2O_3. *J. Catal.* **1982**, *73*, 45–49.

Ceckiewicz, S.; Delmon, B. Cooperation Action of Pt/γ-Al_2O_3 Catalyst and γ-Al_2O_3 Diluent in the Hydrogenation of Benzene. *J. Catal.* **1987**, *108*, 294–303.

Chao, K. C.; Kim, H. Y.; Oliphant, J. L.; Sebastian, H. M.; Simmick, J. J. Phase Equilibrium in Coal Liquefaction Processes; Final Report Prepared for Electric Power Research Institute, Palo Alto, CA, Report No. AP-1593, 1980.

Funk, G. A.; Harold, M. P.; Ng, K. M. Experimental Study of Reaction in a Partially Wetted Catalytic Pellet. *AIChE J.* **1991**, *37* (2), 202–214.

Gutierrez-Ortiz, M. A.; Gonzalez-Macos, M. P.;Arnaiz-Aguilar, S.; Gonzalez-Marcos, J. A.; Gonzalez-Velasco, J. R. Surface Features and Catalytic Performance of Platinum/Alumina Catalysts in Slurry-Phase Hydrogenation. *Ind. Eng. Chem. Res.* **1993**, *32*, 2457–2463.

Harold, M. P.; Ng, K. M. Effectiveness Enhancement and Reactant Depletion in a partially Wetted Catalyst. *AIChE J.* **1987**, *33*, 1448–1465.

Herskowitz, M.; Mosseri, S. Global rates of Reaction in Trickle-Bed Reactors: Effects of Gas and Liquid Flow Rates. *Ind. Eng. Chem. Fundam.* **1983**, *22*, 4–6.

Herskowitz, M.; Smith, J. M. Trickle-Bed Reactors: A Review. *AIChE J.* **1983**, *29* (1), 1–18.

Huang, T.-C.; Kang, B.-C. Kinetic Study of Naphthalene Hydrogenation over Pt/Al_2O_3 Catayst. *Ind. Eng. Chem. Res.* **1995**, *34*, 1140–1148.

Klinken, J. V.; Dongen, R. H. V. Catalyst Dilution for Improved Performance of Laboratory Trickle-Flow Reactors. *Chem. Eng. Sci.* **1980**, *35*, 59–66.

Koussathana, M.; Vanvouka, D.; Economou, H.; Verykios, X. Slurry-Phase Hydrogenation of Aromatic Compounds over Supported Noble Metal Catalysts. *Appl. Catal.* **1991**, *77*, 283–301.

Koussathana, M.; Vamvouka, D.; Tsapatsis, M.; Verykios, X. Hydrogenation of Aromatic Compounds over Noble Metals Dispersed on Doped Titania Carriers. *Appl. Catal. A: Gen.* **1992**, *80*, 99–113.

Lavopa, V.; Satterfield, C. N., Some Effects of Vapor–Liquid Equilibria on Performance of a Trickle-Bed Reactor. *Chem. Eng. Sci.* **1988**, *43* (8), 2175–2180.

Lindsay, R.; Marriott, J. M.; Booth, M.; C. V. Automotive Diesel Fuel: The Balance between Cost-Effectiveness and Environmental Acceptablity. *Pet. Rev.* **1992**, July, 320–325.

Montagna, A. A.; Shah, Y. T. The Rule of Liquid Holdup, Effective Catalyst Wetting, and Backmixing on the Performance of a Trickle Bed Reactor for Residue Hydrodesulfurization. *Ind. Eng. Chem. Process Des. Dev.* **1975**, *14*, 479–483.

Nalitham, V. R.; Guln, J. A.; Tarrer, A. R.; Curtis, C. W. Effect of Phase Behavior on Hydrotreater Performance: Simulation and Experimental Verification. *Ind. Eng. Chem. Process Des. Dev.* **1985**, *24*, 598–607.

Ohe, S. *Computer Aided Data Book of Vapor Pressure*; Data Book Publishing Co.: Tokyo, 1976.

Orozoo, J. M.; Webb, G. The Adsorption and Hydrogenation of Benzene and Toluene on Alumina- Silica-Supported Palladium and Platinum Catalysts. *Appl. Catal.* **1983**, *6*, 67–84.

Patzer, J. F., II; Farrauto, R. J.; Montagna, A. A. Characterization of Coal Liquefaction Catalysts using 1-Methylnaphthalene as a Model Compound. *Ind. Eng. Chem. Process Des. Dev.* **1979**, *18* (4), 625–630.

Ruecker, C. M.; Akgerman, A. Determination of Wetting Efficiencies for a Trickle-Bed Reactor at High Temperatures and Pressures. *Ind. Eng. Chem. Res.* **1987**, *26*, 164–166.

Sakanishi, K.; Ohira, M.; Mochida, I.; Okazaki, H.; Soeda, M. The Reactivities of Polyaromatic Hydrocarbons in Catalytic Hydrogenation over Supported Noble Metal. *Bull. Chem. Soc. Jpn.* **1989**, *62*, 3994–4001.

Sapre, A. V.; Gates, B. C. Hydrogenation of Aromatic Hydrocarbons Catalyzed by Sulfided CoO-MoO_3/γ-Al_2O_3. Reactivities and Reaction Networks. *Ind. Eng. Chem. Process Des. Dev.* **1981**, *20*, 68–73.

Sapre, A. V.; Gates, B. C. Hydrogenation of Biphenyl Catalyzed by Sulfided CoO-MoO_3/γ-Al_2O_3. The Reaction Kinetics. *Ind. Eng. Chem. Process Des. Dev.* **1982**, *21*, 86–94.

Satterfield, C. N. *Trickle-Bed Reactor. AIChE J.* **1975**, *21*, 209–228.

Simth, C. M.; Satterfield, C. N. Some effects of Vapor–Liquid Flow Ratio on Performance of a Trickle-Bed Reactor. *Chem. Eng. Sci.* **1986**, *41* (4), 839–843.

Specchia, V.; Baldi, G. Solid-Liquid Mass Transfer in Cocurrent Two-Phase Flow through Packed Beds. *Ind. Eng. Chem. Process Des. Dev.* **1978**, *17*, 362–367.

Tsai, M. C.; Chen, Y. C.; Kang, B. C.; Wu, J. C.; Leu, L. J. Hydrosulfurization and Hydrodemetalation Reactions of Residue Oils over CoMo/Aluminum Borate Catalysts in a Trickle Bed Reactor. *Ind. Eng. Chem. Res.* **1991**, *30*, 1801–1810.

Ullman, T. L. Investigation of the Effects of Fuel Composition on Heavy-Duty Diesel Engine Emissions. International Fuels and Lubricants Meeting and Exposition, Baltimore, MD, Sept 26–28, 1989; *SAE Pap.* No. 892072.

Weitkamp, A. W. Stereochemistry and Mechanism of Hydrogenation of Naphthalene on Transition Metal Catalysts and Conformational Analysis of the Products. *Adv. Catal.* **1968**, *18*, 1–110.

Wells, P. B. Characterization of the Standard Platinum/Silica Catalyst Europe-1. 5. Chemisorption of Carbon Monoxide and of Oxygen. *Appl. Catal.* **1985**, *18*, 259–272.

Wilson, M. F.; Kriz, J. F. Upgrading of Middle Distillate Fractions of a SynCrude from Athabasca Oil Sands. *Fuel* **1984**, *63*, 190–196.

Wilson, M. F.; Fisher, I. P.; Kriz, J. F. Hydrogenation of Aromatic Compounds in Synthetic Crude Distillates Catalyzed by Sulfided Ni-W/γ-Al_2O_3, *J. Catal.* **1985**, *95*, 155–166.

Received for review June 28, 1994
Revised manuscript received March 30, 1995
Accepted April 30, 1995[⊗]

IE940399Y

[⊗] Abstract published in *Advance ACS Abstracts,* June 15, 1995.